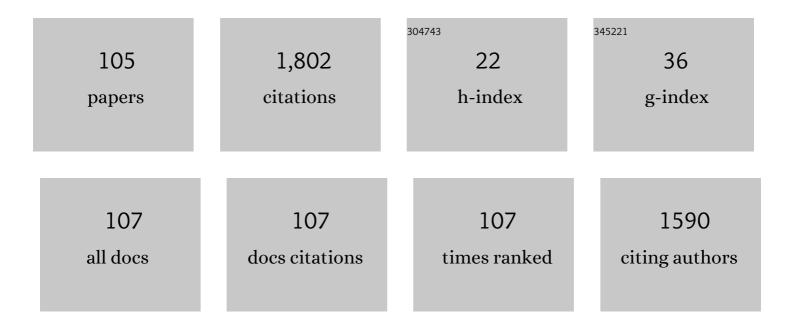
List of Publications by Year in descending order

Source: https://exaly.com/author-pdf/6135976/publications.pdf Version: 2024-02-01



#	Article	IF	CITATIONS
1	Interactions of phase equilibria, jet fluid dynamics and mass transfer during supercritical antisolvent micronization. Chemical Engineering Journal, 2010, 156, 446-458.	12.7	131
2	A shiftedâ€excitation Raman difference spectroscopy (SERDS) evaluation strategy for the efficient isolation of Raman spectra from extreme fluorescence interference. Journal of Raman Spectroscopy, 2016, 47, 198-209.	2.5	70
3	Gas-phase temperature measurement in the vaporizing spray of a gasoline direct-injection injector by use of pure rotational coherent anti-Stokes Raman scattering. Optics Letters, 2004, 29, 247.	3.3	66
4	How Sodium Chloride Salt Inhibits the Formation of CO ₂ Gas Hydrates. Journal of Physical Chemistry B, 2016, 120, 2452-2459.	2.6	65
5	Control of particle size, at micrometric and nanometric range, using supercritical antisolvent precipitation from solvent mixtures: Application to PVP. Chemical Engineering Journal, 2015, 273, 344-352.	12.7	59
6	Raman difference spectroscopy: a non-invasive method for identification of oral squamous cell carcinoma. Biomedical Optics Express, 2014, 5, 3252.	2.9	58
7	Interactions of phase equilibria, jet fluid dynamics and mass transfer during supercritical antisolvent micronization: The influence of solvents. Chemical Engineering Journal, 2012, 203, 71-80.	12.7	57
8	Solute solubility as criterion for the appearance of amorphous particle precipitation or crystallization in the supercritical antisolvent (SAS) process. Journal of Supercritical Fluids, 2012, 66, 350-358.	3.2	52
9	Manipulating the size, the morphology and the polymorphism of acetaminophen using supercritical antisolvent (SAS) precipitation. Journal of Supercritical Fluids, 2013, 82, 230-237.	3.2	49
10	High-pressure pure rotational CARS: comparison of temperature measurements with O2, N2and synthetic air. Journal of Raman Spectroscopy, 2003, 34, 932-939.	2.5	46
11	Laser-induced fluorescence of ketones at elevated temperatures for pressures up to 20 bars by using a 248 nm excitation laser wavelength: experiments and model improvements. Applied Optics, 2006, 45, 4982.	2.1	40
12	Supercritical drying of aerogel: In situ analysis of concentration profiles inside the gel and derivation of the effective binary diffusion coefficient using Raman spectroscopy. Journal of Supercritical Fluids, 2016, 108, 1-12.	3.2	39
13	Supercritical antisolvent micronization of PVP and ibuprofen sodium towards tailored solid dispersions. Journal of Supercritical Fluids, 2014, 89, 16-27.	3.2	35
14	Investigation of the combustion process in an auxiliary heating system using dual-pump CARS. Journal of Raman Spectroscopy, 2006, 37, 633-640.	2.5	31
15	Deconvolution of Raman spectra for the quantification of ternary highâ€pressure phase equilibria composed of carbon dioxide, water and organic solvent. Journal of Raman Spectroscopy, 2014, 45, 246-252.	2.5	28
16	Model development for sc-drying kinetics of aerogels: Part 1. Monoliths and single particles. Journal of Supercritical Fluids, 2018, 140, 415-430.	3.2	27
17	Analysis of the supercritical antisolvent mechanisms governing particles precipitation and morphology by in situ laser scattering techniques. Chemical Engineering Journal, 2011, 173, 258-258.	12.7	26
18	Laser analyses of mixture formation and the influence of solute on particle precipitation in the SAS process. Journal of Supercritical Fluids, 2009, 50, 265-275.	3.2	25

#	Article	IF	CITATIONS
19	Non-invasive quantification of phase equilibria of ternary mixtures composed of carbon dioxide, organic solvent and water. Journal of Supercritical Fluids, 2013, 84, 146-154.	3.2	25
20	Surfactant-free CO ₂ -based microemulsion-like systems. Chemical Communications, 2014, 50, 8215-8218.	4.1	25
21	Hydrogen Bond Networks in Binary Mixtures of Water and Organic Solvents. Journal of Physical Chemistry B, 2019, 123, 4425-4433.	2.6	25
22	CO2 partial density distribution during high-pressure mixing with ethanol in the supercritical antisolvent process. Journal of Supercritical Fluids, 2009, 48, 195-202.	3.2	24
23	Gas mixing analysis by simultaneous Raman imaging and particle image velocimetry. Optics Letters, 2009, 34, 3122.	3.3	24
24	High-pressure microfluidics for the investigation into multi-phase systems using the supercritical fluid extraction of emulsions (SFEE). Journal of Supercritical Fluids, 2012, 65, 78-86.	3.2	22
25	Recent Advances in Experimental Techniques forÂFlow and Mass Transfer Analyses in Thermal Separation Systems. Chemie-Ingenieur-Technik, 2020, 92, 926-948.	0.8	22
26	Two-dimensional Raman mole-fraction and temperature measurements for hydrogen-nitrogen mixture analysis. Applied Optics, 2009, 48, B57.	2.1	21
27	A Raman spectroscopic method for the determination of high pressure vapour liquid equilibria. Fluid Phase Equilibria, 2013, 360, 265-273.	2.5	21
28	Investigation of CO2 sorption in molten polymers at high pressures using RamanÂline imaging. Polymer, 2013, 54, 812-818.	3.8	20
29	The lag between micro- and macro-mixing in compressed fluid flows. Chemical Engineering Science, 2017, 163, 105-113.	3.8	20
30	Quantification of mixture composition, liquid-phase fraction and - temperature in transcritical sprays. Journal of Supercritical Fluids, 2020, 159, 104777.	3.2	20
31	Simultaneous laser-induced fluorescence and Raman imaging inside a hydrogen engine. Applied Optics, 2009, 48, 6643.	2.1	19
32	Quantification of the mass transport in a two phase binary system at elevated pressures applying Raman spectroscopy: Pendant liquid solvent drop in a supercritical carbon dioxide environment. International Journal of Heat and Mass Transfer, 2013, 62, 729-740.	4.8	19
33	Influence of Sodium Chloride on the Formation and Dissociation Behavior of CO ₂ Gas Hydrates. Journal of Physical Chemistry B, 2017, 121, 8330-8337.	2.6	19
34	In situ optical monitoring of the solution concentration influence on supercritical particle precipitation. Journal of Supercritical Fluids, 2010, 55, 282-291.	3.2	18
35	Determination of Vapor–Liquid Equilibrium Data in Microfluidic Segmented Flows at Elevated Pressures Using Raman Spectroscopy. Analytical Chemistry, 2015, 87, 8165-8172.	6.5	18
36	Vapor-liquid-equilibria of fuel-nitrogen systems at engine-like conditions measured with Raman spectroscopy in micro capillaries. Fuel, 2019, 238, 312-319.	6.4	18

#	Article	IF	CITATIONS
37	Simultaneous determination of the composition and temperature gradients in the vicinity of boiling bubbles in liquid binary mixtures using oneâ€dimensional Raman measurements. Journal of Raman Spectroscopy, 2011, 42, 195-200.	2.5	17
38	Microfluidic investigation into mass transfer in compressible multi-phase systems composed of oil, water and carbon dioxide at elevated pressure. Journal of Supercritical Fluids, 2013, 84, 121-131.	3.2	17
39	Breast Tumor Analysis Using Shifted-Excitation Raman Difference Spectroscopy (SERDS). Technology in Cancer Research and Treatment, 2018, 17, 153303381878253.	1.9	17
40	Observation of liquid solution volume expansion during particle precipitation in the supercritical CO2 antisolvent process. Journal of Supercritical Fluids, 2011, 56, 121-124.	3.2	16
41	Solubility of Paracetamol and Polyvinylpyrrolidone in Mixtures of Carbon Dioxide, Ethanol, and Acetone at Elevated Pressures. Journal of Chemical & Engineering Data, 2013, 58, 1054-1061.	1.9	16
42	In Situ Raman Analysis of CO2—Assisted Drying of Fruit-Slices. Foods, 2017, 6, 37.	4.3	16
43	Refinement of spectra using a deep neural network: Fully automated removal of noise and background. Journal of Raman Spectroscopy, 2021, 52, 723-736.	2.5	16
44	Imaging the supersaturation in high-pressure systems for particle generation. Chemical Engineering Journal, 2011, 168, 896-902.	12.7	15
45	Liquid phase temperature determination in dense water sprays using linear Raman scattering. Optics Express, 2014, 22, 7962.	3.4	15
46	Shining light on low-temperature methanol aqueous-phase reforming using homogeneous Ru-pincer complexes – operando Raman-GC studies. Reaction Chemistry and Engineering, 2017, 2, 390-396.	3.7	15
47	Pressure-Responsive, Surfactant-Free CO2-Based Nanostructured Fluids. ACS Nano, 2017, 11, 10774-10784.	14.6	15
48	Phase-specific Raman spectroscopy for fast segmented microfluidic flows. Lab on A Chip, 2014, 14, 2910-2913.	6.0	14
49	Simultaneous Raman and elastic light scattering imaging for particle formation investigation. Optics Letters, 2010, 35, 2553.	3.3	12
50	Lycopene solubility in mixtures of carbon dioxide and ethyl acetate. Journal of Supercritical Fluids, 2013, 75, 6-10.	3.2	12
51	One-dimensional Raman spectroscopy and shadowgraphy for the analysis of the evaporation behavior of acetone/water drops. International Journal of Heat and Mass Transfer, 2015, 89, 406-413.	4.8	12
52	In situ Raman quantification of the dissolution kinetics of carbon dioxide in liquid solutions during a dense phase and ultrasound treatment for the inactivation of Saccharomyces cerevisiae. Journal of Supercritical Fluids, 2016, 111, 104-111.	3.2	12
53	Protein gel shrinkage during solvent exchange: Quantification of gel compaction, mass transfer and compressive strength. Food Hydrocolloids, 2021, 120, 106916.	10.7	12

 $_{54}$ Vapor pressures and latent heats of vaporization of Poly(oxymethylene) Dimethyl Ethers (OME3 and) Tj ETQq0 0 0 $_{64}^{rgBT}$ /Overlock 10 Tf

#	Article	IF	CITATIONS
55	Injection of ethanol into supercritical CO_2: Determination of mole fraction and phase state using linear Raman scattering. Optics Express, 2007, 15, 8377.	3.4	11
56	Raman mixture composition and flow velocity imaging with high repetition rates. Optics Express, 2010, 18, 24579.	3.4	11
57	In situ monitoring of the acetylene decomposition and gas temperature at reaction conditions for the deposition of carbon nanotubes using linear Raman scattering. Optics Express, 2010, 18, 18223.	3.4	10
58	Flow field characterization in a vertically oriented cold wall CCVD reactor by particle image velocimetry. Chemical Engineering Journal, 2012, 184, 315-325.	12.7	10
59	A Raman technique applicable for the analysis of the working principle of promoters and inhibitors of gas hydrate formation. Journal of Raman Spectroscopy, 2015, 46, 1145-1149.	2.5	10
60	On the unexpected non-monotonic profile of specific volume observed in PCL/CO2 solutions. Polymer, 2015, 56, 252-255.	3.8	10
61	Online monitoring of the supercritical CO2 extraction of hop. Journal of Supercritical Fluids, 2018, 133, 139-145.	3.2	10
62	Vector casting for noise reduction. Journal of Raman Spectroscopy, 2020, 51, 731-743.	2.5	10
63	Optical diagnosis of oral cavity lesions by label-free Raman spectroscopy. Biomedical Optics Express, 2021, 12, 836.	2.9	10
64	Simultaneous in situ Raman monitoring of the solid and gas phases during the formation and growth of carbon nanostructures inside a cold wall CCVD reactor. Carbon, 2014, 78, 164-180.	10.3	9
65	Simultaneous Analysis of the Dispersed Liquid and the Bulk Gas Phase of Water Sprays Using Raman Spectroscopy. Applied Spectroscopy, 2016, 70, 1055-1062.	2.2	9
66	Prospects: Facing current challenges in high pressure high temperature process engineering with in situ Raman measurements. Journal of Supercritical Fluids, 2018, 134, 80-87.	3.2	9
67	In situ analysis of aerosols by Raman spectroscopy – Crystalline particle polymorphism and gas-phase temperature. Journal of Aerosol Science, 2018, 126, 143-151.	3.8	9
68	In situ Raman-analysis of supercritical carbon dioxide drying applied to acellular esophageal matrix. Journal of Supercritical Fluids, 2017, 128, 194-199.	3.2	8
69	TEMPERATURE CHARACTERISTICS IN A FLASH ATOMIZATION PROCESS. Atomization and Sprays, 2016, 26, 1337-1359.	0.8	8
70	Supercritical Antisolvent Particle Precipitation: In Situ Optical Investigations. Chemical Engineering and Technology, 2010, 33, 35-38.	1.5	7
71	In situ quantification of minor compounds in pressurized carbon dioxide using Raman spectroscopy. Journal of Supercritical Fluids, 2013, 82, 263-267.	3.2	7
72	Interaction of Matter and Electromagnetic Radiation. Supercritical Fluid Science and Technology, 2015, 7, 41-192.	0.5	7

#	Article	IF	CITATIONS
73	In Situ Raman Monitoring of the Formation and Growth of Carbon Nanotubes via Chemical Vapor Deposition. Procedia Engineering, 2015, 102, 190-200.	1.2	7
74	Raman Line Imaging of Poly(ε-caprolactone)/Carbon Dioxide Solutions at High Pressures: A Combined Experimental and Computational Study for Interpreting Intermolecular Interactions and Free-Volume Effects. Journal of Physical Chemistry B, 2016, 120, 9115-9131.	2.6	7
75	Raman Spectroscopic Study of the Effect of Aqueous Salt Solutions on the Inhibition of Carbon Dioxide Gas Hydrates. Journal of Physical Chemistry B, 2019, 123, 2354-2361.	2.6	6
76	Use of Bentonite and Organic Binders in the Briquetting of Particulate Residues from the Midrex Process for Improving the Thermal Stability and Reducibility of the Briquettes. Steel Research International, 2021, 92, 2100210.	1.8	6
77	Temperature determination of superheated water vapor by rotational-vibrational Raman spectroscopy. Optics Letters, 2018, 43, 4477.	3.3	5
78	Vapor–Liquid Equilibria of Mixtures Containing Ethanol, Oxygen, and Nitrogen at Elevated Pressure and Temperature, Measured with <i>In Situ</i> Raman Spectroscopy in Microcapillaries. Journal of Chemical & Engineering Data, 2020, 65, 3373-3383.	1.9	5
79	The influence of temperature and pressure on macro- and micro-mixing in compressed fluid flows; mixing of carbon dioxide and ethanol above their mixture critical pressure. Journal of Supercritical Fluids, 2021, 167, 105036.	3.2	5
80	Shadowgraph and Schlieren Techniques. Supercritical Fluid Science and Technology, 2015, , 283-312.	0.5	4
81	In situ measurement of drug transport in porous silica gel. Microporous and Mesoporous Materials, 2018, 260, 17-23.	4.4	4
82	Growth Rate of Pressureâ€Induced Triolein Crystals. JAOCS, Journal of the American Oil Chemists' Society, 2019, 96, 25-33.	1.9	4
83	Shifted-excitation rotational Raman spectroscopy and Bayesian inference for in situ temperature and composition determination in laminar flames. Journal of Quantitative Spectroscopy and Radiative Transfer, 2020, 249, 106996.	2.3	4
84	Anomalous swelling of molten PCL/scCO2 solutions. , 2014, , .		3
85	High Pressure: Fellow and Opponent of Spectroscopic Techniques. Supercritical Fluid Science and Technology, 2015, , 1-40.	0.5	3
86	A fast and remote screening method for sub-micro-structuration in pressurized mixtures containing water and carbon dioxide. Journal of Supercritical Fluids, 2019, 152, 104555.	3.2	3
87	Non-saturated mixture densities of the binary systems of carbon dioxide and the organic solvents ethanol, acetone, acetonitrile and dimethyl sulfoxide from 6-12 MPa. Fluid Phase Equilibria, 2021, 549, 113201.	2.5	3
88	Application, characterisation and economic assessment of brewers' spent grain and liquor. Journal of the Institute of Brewing, 2022, 128, 96-108.	2.3	3
89	Increase of the stimulated Raman scattering threshold at droplets by spectral broadening of nanosecond laser pulses. Journal of Raman Spectroscopy, 2012, 43, 1935-1940.	2.5	2
90	Laser-Induced Fluorescence (LIF) and Phosphorescence (LIP) Techniques. Supercritical Fluid Science and Technology, 2015, 7, 313-345.	0.5	2

#	Article	IF	CITATIONS
91	Raman Thermometry in Water, Ethanol, and Ethanol/Nitrogen Mixtures from Ambient to Critical Conditions. Analytical Chemistry, 2019, 91, 1043-1048.	6.5	2
92	CO2 induced gelation of amidated pectin solutions: Impact of viscosity and gel formation. Chemical Engineering Research and Design, 2022, 180, 153-163.	5.6	2
93	Investigations on Strategic Element Recovery by an Underground Membrane Pilot Plant from In-Situ Extracted Bioleaching Solutions. Minerals (Basel, Switzerland), 2022, 12, 46.	2.0	2
94	Absorption Spectroscopy. Supercritical Fluid Science and Technology, 2015, 7, 347-366.	0.5	1
95	Analysis of the Dissolution of CH4/CO2-Mixtures into Liquid Water and the Subsequent Hydrate Formation via In Situ Raman Spectroscopy. Energies, 2020, 13, 793.	3.1	1
96	Rotational Raman spectroscopy for in situ temperature and composition determination in reactive flows. , 2019, , .		1
97	Filter-coated Raman fiber bundle probe and deep neural networks for oral cancer diagnostics. , 2021, ,		1
98	Sustainable value added material use of occurring by-products from sugar and rice production in Vietnam. Science of the Total Environment, 2022, 835, 155414.	8.0	1
99	Vapor-Liquid equilibria of the systems 1-octanol/nitrogen and 1-octanol/oxygen at pressures from 3 to 9ÂMPa and temperatures up to 613ÂK – Measured in a microcapillary with Raman spectroscopy. Fuel, 2022, 323, 124352.	6.4	1
100	Optische inâ€situâ€Untersuchungen der Partikelbildung im überkritischen Antisolventâ€Prozess. Chemie-Ingenieur-Technik, 2009, 81, 1453-1457.	0.8	0
101	Measurement of Concentration and Temperature Gradients at Binary Mixture Boiling Bubbles. , 2010, , .		0
102	Raman Spectroscopy From an Engineering Point of View. Supercritical Fluid Science and Technology, 2015, 7, 193-281.	0.5	0
103	Pressure drop particle precipitation from a quasi-incompressible, ternary and liquid mixture. Journal of Supercritical Fluids, 2021, 175, 105301.	3.2	0
104	Development of Imaging Laser Diagnostics for the Validation of LE-Simulations of Flows with Heat and Mass Transfer. Notes on Numerical Fluid Mechanics and Multidisciplinary Design, 2009, , 175-184.	0.3	0
105	Analysis of Mechanisms for PVP-Active-Agent Formulation as in Supercritical Antisolvent Spray Process. , 2016, , 987-1035.		0